*30th EPS Conference on Contr. Fusion and Plasma Phys., St. Petersburg, 7-11 July 2003 ECA Vol. **27A**, P-4.17*

# OPTIMIZED POLOIDAL PSEUDOSYMMETRY FOR TOROIDAL SYSTEMS

V.D. Shafranov[1], W.A. Cooper[2], M.Yu. Isaev[1], M.I. Mikhailov[1], J. Nührenberg[3], M.A. Samitov[1], A.A. Skovoroda[1], A.A. Subbotin[1], R. Zille[3]

[1] Russian Research Centre "Kurchatov Institute", Moscow, Russia

[2] Centre de Recherches en Physique des Plasmas, Association Euratom-Confédération Suisse, Ecole Polytechnique Fédérale de Lausanne, Switzerland

[3] Max-Planck-Institut für Plasmaphysik, IPP-EURATOM Association, Germany

**Abstract**

The numerical optimization of stellarator systems from the viewpoint of plasma equilibrium, stability and particle confinement has shown that rather good properties can be achieved in configurations having most of the $B$ contours closed around a magnetic axis of helical form. Note that the optimized stellarator W7-X (see, e.g., Ref.[1]) belongs just to this type. The possibility to fulfill the quasi-isodynamicity condition in such type of stellarators with poloidal closed mod-$B$ contours was analyzed in Ref. [2] for deeply to moderately trapped particles. In Ref. [3] it was shown for moderate number of periods $N = 6$, and aspect ratio per period $A_p = R/Na \sim 2$ ($R, a$ are the major and averaged minor radii of toroidal system), that this condition can be extended to all reflected particles. It is worth to emphasize that the configurations considered have no symmetric analogue even for a large number of periods and high aspect ratio. Thus, the confinement properties of such kind of stellarators for large number of periods should be investigated step by step. In the present report, some results are presented for a nine-period system.

**Introduction**

In the present paper, the stellarator configurations with mod-$B$ = constant lines in the poloidal direction on the magnetic surfaces are considered. For such type of magnetic configurations, the improvement of the reflected particle confinement can be achieved by optimization of the contours of the second adiabatic invariant, $\mathcal{J} = \int v_\parallel dl = \mathcal{J}(s)$, to be constant on magnetic surfaces through the poloidal closure of these contours ($s$ is normalized toroidal flux; $s$=1 on the boundary). In Ref. [2], where this condition was named quasi-isodynamicity, the possibility was shown to satisfy it for deeply to moderately deeply trapped particles. In Ref. [3] it was demonstrated by numerical optimization that this condition can be satisfied for all reflected particles. A six-period configuration found with finite $\beta \approx 5\%$ possesses good collisionless fast-particle confinement. In addition, it was shown that the requirement of good particle confinement is well compatible with local interchange-mode stability conditions.

In the configurations of the type considered, the bumpy component of the magnetic field strength is necessary to create mod-$B$ = constant lines in the poloidal direction on the magnetic surfaces. To avoid the appearance of islands in the $B$ = constant lines on the magnetic surfaces, the longitudinal variation of $B$ should be larger then the poloidal variation of $B$ connected with the curvature of the magnetic axis. In the cross-sections with magnetic field strength extrema, the toroidal variation of $B$ is zero and cannot compensate finite poloidal variation. Thus in these cross-sections the magnetic axis curvature should be zero. Nevertheless, significant curvature of the magnetic axis is needed in most parts of the system for the creation of a vacuum magnetic well. Note

that the magnetic well can be realized in systems with poloidal closed $B$ contours due to the helical-type structure of the magnetic axis. Thus, it is interesting to investigate the confinement properties of such kind of stellarators for large number of periods. As a step in this direction, a nine-period system is considered in the present paper. As one can expect, the secondary currents are smaller in the nine-period configuration in comparison with the previously optimized six-period system. Because of this, it becomes possible to find a configuration with an increased value of plasma pressure, $< \beta >= 10\%$.

**Results of numerical optimization**

The numerical optimization was performed on the supercomputers Himiko (Germany) and Prometeo (Switzerland) by using the equilibrium code VMEC [4], the code JMC [5] for transition to magnetic (Boozer) coordinates and the codes for calculation of different target functions. The direct particle drift orbit calculation was performed with the MCT code [6].

*Starting configuration and choice of the target functions*

The boundary magnetic surface of the earlier six-period configuration [3] with $< \beta >= 5\%$ was adapted to nine periods with a corresponding change of the aspect ratio from 12 to about 22. The transformed configuration had very small secondary currents and almost zero or even inward magnetic axis shift both for zero and high enough $\beta$, and possesses a vacuum magnetic well (except in the near-boundary region). This configuration was optimized at $< \beta >= 10\%$ by using the conditions of pseudosymmetry [7], closure of the second adiabatic invariant contours [8] and Mercier and resistive mode stability criteria.

*The structure of the surfaces $B$ = constant and particle confinement*

Fig. 1 shows a 3D view of the boundary magnetic surface of the optimized $N = 9$ configuration. The color here marks the value of the magnetic field strength on the boundary. It is seen that the lines $B$ = constant go around the magnetic axis (see, also, Fig. 2). The structure of the surfaces $B$ = constant is shown in Fig. 3 along with two magnetic surfaces. The reflected particles are trapped between the corresponding surfaces $B$ = constant, i.e. inside the system period. Fig. 4 shows the contours of the second adiabatic invariants in polar representation $\sqrt{s}, \theta_B$ for a set of increasing values of $B_{reflect}$.

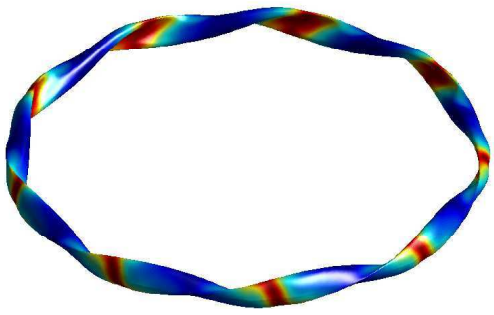

Fig. 1. 3D view of optimized nine-period configuration. The color defines the value of the magnetic field strength.

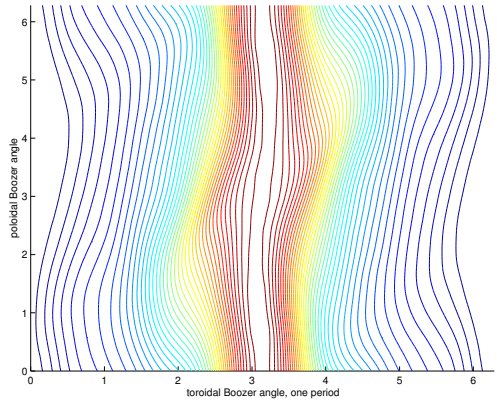


Fig. 2. Contours of $B$ on the magnetic surface with $s = 0.25$ (one half of minor plasma radius) for the optimized configuration.

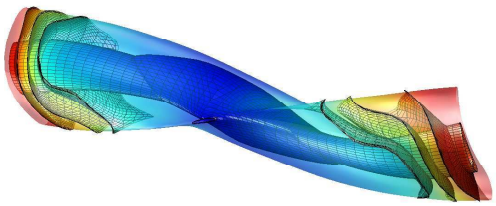

Fig. 3. The magnetic surfaces are intersected by surfaces $B$ = constant. One system period is shown.

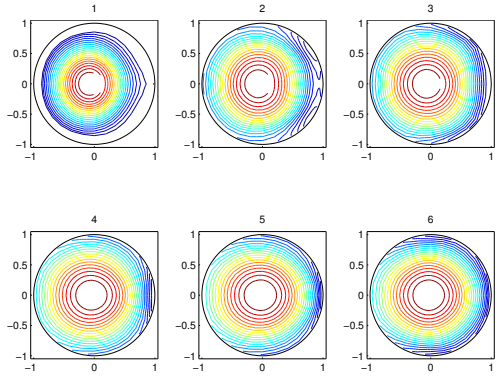


Fig. 4. Contours of the second adiabatic invariant in polar representation (normalized plasma radius $\sqrt{s}$, poloidal angle $\theta_B$) for increased set of $B_{reflect}$

An example of projection of the trapped $\alpha$-particle drift trajectory along the magnetic field lines on the surface $\zeta_B$ = constant is shown in Fig. 5. Here the color marks the value of the parallel velocity. The quality of the fast $\alpha$-particle confinement was checked by direct calculation of the collisionless guiding centre orbits of 1000 particles during 1 sec and the results of these calculations are shown in Fig. 6. The following power plant-size normalization was used: $B_0 = 5$T and a plasma volume of 1000 $m^3$. It is seen that there is almost zero loss for particles started at 1/2 of the plasma minor radius, while about 10% of particles started at 2/3 of the plasma radius escaped from the plasma, despite the closure of most of the $\mathcal{J}$ contours.

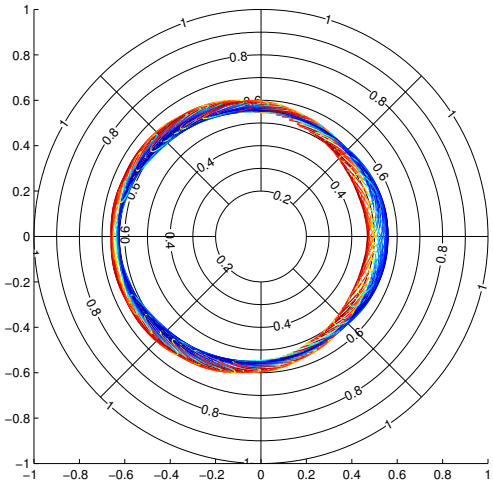

Fig. 5. The projection of $\alpha$-particle collisionless guiding centre trajectory on the cross-section $\zeta_B$ = constant. The colours define the sign and the value of the parallel velocity (red corresponds to positive direction, blue means negative direction).

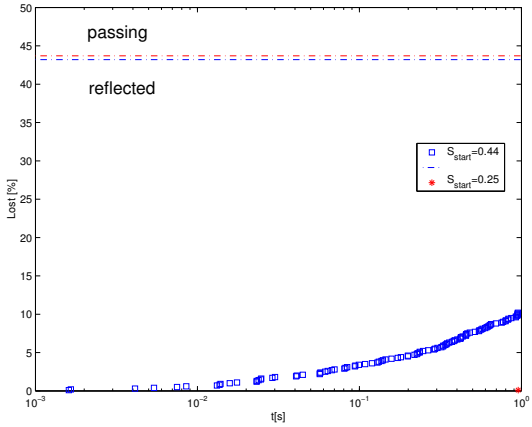


Fig. 6. Collisionless $\alpha$-particle confinement in the optimized configuration as a function of the time of flight. Particles are started at $s_{start} = 0.25$ (red, 1/2 of the plasma radius) and at $s_{start} = 0.44$ (blue, 2/3 of the plasma radius); the dashed lines show the fractions of the reflected particles.

*Equilibrium and stability properties of the optimized configuration*

Fig. 7 shows the cross-sections of the optimized configuration in the beginning, one quarter and one half of a period and radial profiles of the rotational transform, magnetic well and plasma pressure for almost zero $\beta$ (top) and $< \beta >= 10\%$ (bottom).

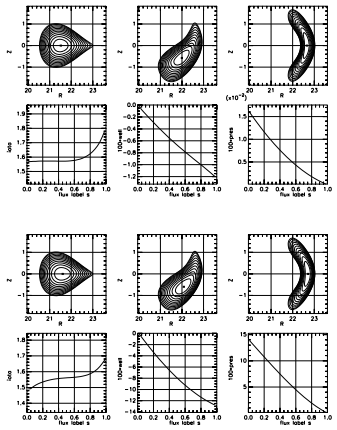

Fig. 7. Cross-sections of optimized configurations for $< \beta >= 0$ and $< \beta >= 10\%$.

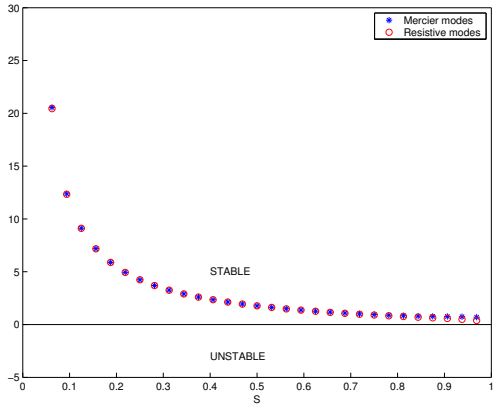


Fig. 8. Mercier and resistive mode stability of optimized configurations.

It is seen that the vacuum configuration has a magnetic well of the order of 1%. The transition from zero $\beta$ to $< \beta >= 10\%$ increases the shift of the magnetic surfaces only slightly, the rotational transform profile is not changed very much, too. Fig. 8 demonstrates that Mercier and resistive modes are stable in this optimized configuration.

**Conclusion.** It is shown by numerical optimization for configurations with mod-$B$ = constant lines in the poloidal direction on the magnetic surfaces that increasing the number of plasma periods and aspect ratio permits to realize good collisionless particle confinement properties and to satisfy the local interchange-mode stability criteria for a sufficiently high $< \beta >$ value. In spite of the small toroidal curvature of the magnetic axis, a vacuum magnetic well can be created due to the non-planar behavior of the magnetic axis.

**Acknowledgments** This work was supported by INTAS Grant No 99-00592; Russian-Germany agreement WTZ-RUS-01/581; Russian Federal program on support of leading scientific school researches, Grant No 2024.2003.2; Russian Fund for Basic Research, Grant No 03-02-16768; Fonds National Suisse de la Recherche Scientifique, Euratom; Department of atomic science and technology, Minatom RF. One of the authors (M.I.M) would like to thank Prof. K. Yamazaki for helpful discussions during his stay in NIFS, Japan.

**References**

[1] W.Lotz, J.Nührenberg, C.Schwab, 1991 Proc. 13th Int. Conf. on Plasma Phys. and Contr. Nucl. Fus. Res. 1990 (Washington, 1990) vol 2 (Vienna: IAEA) 603.

[2] S.Gori, W.Lotz, J.Nührenberg, Theory of Fusion Plasmas (International School of Plasma Physics), Bologna: SIF (1996) 335.

[3] M.I.Mikhailov, V.D.Shafranov, A.A.Subbotin et.al., Nuclear Fusion **42** (2002) L23.

[4] S.P.Hirshman and O.Betancourt, J. of Comput. Physics **96** (1991) 99.

[5] J.Nührenberg, R.Zille, Theory of Fusion Plasmas (Varenna 1987), Editrice Compositori, Bologna (1988) 3.

[6] R.H.Fowler, J.A.Rome, J.F.Lyon, Phys. Fluids **28** (1985) 338.

[7] M.I.Mikhailov, W.A.Cooper, M.Yu.Isaev et. al. Theory of Fusion Plasmas (International School of Plasma Physics), Bologna: SIF (1998) 185.

[8] A.A.Subbotin, M.I.Mikhailov, J.Nührenberg et.al. 28th EPS Conf. on Controlled Fusion and Plasma Physics, Funchal, Portugal, 2001 (http://www.cfn.ist.utl.pt/EPS2001/fin).